

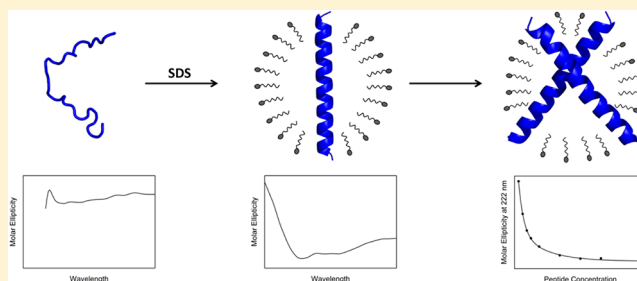
# Membrane Mimetics Induce Helix Formation and Oligomerization of the Chloride Intracellular Channel Protein 1 Transmembrane Domain

Bradley Peter, Nomxolisi Chloë Mina-Liz Ngubane, Sylvia Fanucchi, and Heini W. Dirr\*

Protein Structure-Function Research Unit, School of Molecular and Cell Biology, University of the Witwatersrand, Johannesburg 2050, South Africa

## Supporting Information

**ABSTRACT:** Chloride intracellular channel protein 1 (CLIC1) is a dual-state protein that can exist either as a soluble monomer or in an integral membrane form. The transmembrane domain (TMD), implicated in membrane penetration and pore formation, comprises helix  $\alpha 1$  and strand  $\beta 2$  of the N-domain of soluble CLIC1. The mechanism by which the TMD binds, inserts, and oligomerizes in membranes to form a functional chloride channel is unknown. Here we report the secondary, tertiary, and quaternary structural changes of the CLIC1 TMD as it partitions between an aqueous and membrane-mimicking environment. A synthetic 30-mer peptide comprising the TMD was examined in 2,2,2-trifluoroethanol, sodium dodecyl sulfate (SDS) micelles, and 1-palmitoyl-2-oleoyl-*sn*-glycero-3-phosphocholine (POPC) liposomes using far-ultraviolet circular dichroism and fluorescence spectroscopy. Data obtained in the presence of SDS micelles and POPC liposomes show that Trp35 and Cys24 have reduced solvent accessibility, indicating that the peptide adopts an inserted orientation. The peptide assumes a helical structure in the presence of these mimetics, consistent with its predicted membrane conformation. This acquisition of secondary structure is concentration-dependent, suggesting an oligomerization event. Stable dimeric and trimeric species were subsequently identified using SDS–polyacrylamide gel electrophoresis. We propose that, in the vicinity of membranes, the mixed  $\alpha/\beta$  TMD in CLIC1 rearranges to form a helix that then likely dimerizes via noncovalent helix–helix interactions to form a membrane-competent protopore complex. Such oligomerization would be essential for forming a functional ion channel, given that each CLIC1 monomer possesses only a single TMD. This work highlights the central role of the TMD in CLIC1 function: It is capable of promoting membrane insertion and dimerization in the absence of the C-domain and large portions of the N-domain.



Membrane proteins play key physiological roles, accounting for nearly one-quarter of eukaryotic proteins and constituting approximately 50% of all current drug targets.<sup>1</sup> Despite their importance, the mechanisms by which membrane proteins bind and insert into membranes remain elusive. The two-state folding model proposed by Popot and Engelman<sup>2</sup> and the modified two-state model of White and Wimley<sup>3</sup> have been used to explain these interactions. Proteins capable of adopting multiple stable native states present an intriguing variation to these schemes. These proteins undergo large-scale structural rearrangements upon association with the lipid bilayer, resulting in the spontaneous conversion from a water-soluble to a membrane-bound form.<sup>4</sup> Structural metamorphism is a widely observed phenomenon and occurs in many bacterial pore-forming toxins,<sup>5,6</sup> apoptotic proteins,<sup>7</sup> and the eukaryotic chloride intracellular channel (CLIC) protein family.<sup>8</sup>

In their reduced monomeric state, the CLIC proteins adopt a topology similar to that of the GST superfamily, with a thioredoxin N-domain and an all- $\alpha$ -helical C-domain (Figure 1).<sup>9</sup> CLICs are unique among all eukaryotic ion channels in that they are dimorphic and can exist in either a soluble or membrane-bound form.<sup>9</sup> Unlike typical ion channels, most CLIC proteins lack a signal sequence and remain in the

cytoplasm, spontaneously inserting into membranes under certain environmental conditions.<sup>8,10</sup> The structural basis of the soluble–membrane transition of CLIC1 is poorly understood but is thought to involve the exposure of putative trans-membrane (PTM) domains.

Sequence comparisons between members of the vertebrate CLIC family identify two PTM regions of sufficient hydrophobicity.<sup>11</sup> The first comprises  $\alpha$ -helix 1 and  $\beta$ -strand 2 of the N-domain (Figure 1A), while the second encompasses  $\alpha$ -helix 6 of the C-domain.<sup>12</sup> The former was initially thought to be too stable to readily unfold to yield a membrane-interacting domain, given its evolutionary relationship with the thioredoxin superfamily.<sup>11</sup> However, studies using proteinase K digestion,<sup>13</sup> FLAG epitopes,<sup>14</sup> and terminally directed antibodies<sup>15</sup> of membrane-inserted CLIC1 showed that the C-domain remains cytoplasmic while the N-terminus inserts into the membrane with Cys24 localized at the trans face of the membrane.

Received: March 5, 2013

Revised: April 2, 2013

Published: April 2, 2013



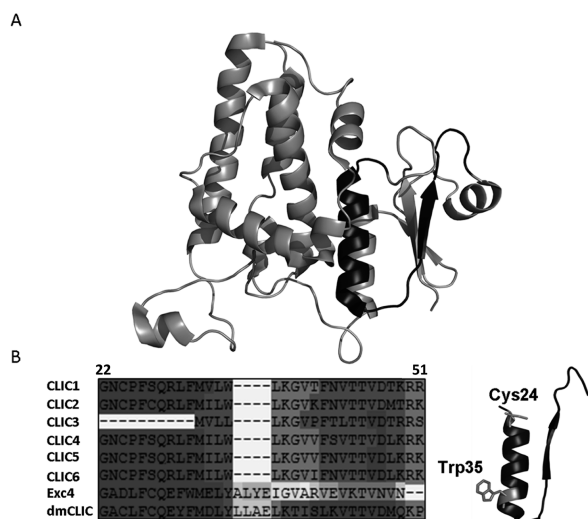


**Figure 1.** Structure and sequence conservation of the CLIC1 TMD. (A) The CLIC1 TMD (black) comprises residues 24–46, which include most of helix  $\alpha 1$  and strand  $\beta 2$  of the N-domain. (B) This region, pictured, shows strong sequence conservation across the vertebrate CLICs as well as the invertebrate homologues Exc4 (*Caenorhabditis elegans*) and dmCLIC (*Drosophila melanogaster*).

On the basis of this evidence, coupled with results from hydrophobicity plots and the TMPred algorithm, Berry and Hobert<sup>16</sup> proposed that the CLIC1 transmembrane domain (TMD) was a 23-residue fragment comprising residues 24–46, a region that is highly conserved among CLIC proteins (Figure 1B). Recent studies by Goodchild et al.<sup>17</sup> used fluorescence quenching to confirm that Trp35 of the N-domain is indeed located within the plasma membrane in the membrane-bound state. The proposed CLIC1 TMD is of sufficient length to span the membrane and contains many conserved features characteristic of transmembrane domains,<sup>18–20</sup> including a central span of predominantly apolar residues and charged residues at the membrane interface. Although the structure of the membrane-bound form of CLIC1 is yet to be determined, the transmembrane segment is predicted to be helical,<sup>8,21,22</sup> with the AGADIR algorithm showing that this region has a high helical propensity.<sup>22</sup>

For the TMD to be exposed to the membrane, a large structural rearrangement of the CLIC1 N-domain is required. It has been proposed that the  $\beta 1\alpha 1\beta 2$  motif detaches from the rest of the protein and refolds into the transmembrane conformation. This is presumably triggered by (i) lowered stability<sup>22</sup> and enhanced flexibility<sup>23</sup> at low pH, (ii) oxidation,<sup>8,17</sup> or (iii) the polarity of the membrane interface. This, however, remains speculative in the absence of structural data.

To improve our understanding of how CLIC1 refolds and inserts into membranes, we need to understand how the structure of the functionally relevant TMD behaves in a membrane environment. In this study, we examined the secondary, tertiary, and quaternary structural changes of the CLIC1 TMD as it partitions between an aqueous and membrane-mimicking environment. Our results show that the TMD undergoes structural modifications in a micellar environment, including the acquisition of helical secondary structure and dimerization. Fluorescence quenching of Trp35 shows that the acquisition of secondary structure correlates with the insertion of the peptide into SDS micelles and POPC

liposomes, although whether these processes occur sequentially or in parallel is yet to be determined. This work shows that the TMD alone is sufficient to promote membrane insertion in the absence of a signal peptide, the C-domain, and the remainder of the N-domain. Similarly, the TMD is capable of forming stable, noncovalent dimers in the absence of the N- and C-domains.

## MATERIALS AND METHODS

**Peptide Design and Synthesis.** The 30-residue CLIC1 TMD peptide (GNCPSQRLFMVLWLKGVTFNVTVDTKRR) containing a carboxylated amino terminus and an amidated carboxyl terminus was synthesized using a solid phase continuous flow system by GL Biochem (Shanghai, China). Its purity was determined to be >95% using high-performance liquid chromatography.

**Sample Preparation.** For conformational studies, the hydrophobic peptide was solubilized in 100% (v/v) methanol to yield a 1 mM stock solution. For SDS work, the peptide was incorporated into SDS micelles as previously described.<sup>24</sup> Briefly, the peptide was added to 20 mM sodium phosphate buffer containing 15 mM SDS to yield a final peptide concentration of 5–50  $\mu$ M. Samples were then vortexed, freeze-dried, and rehydrated in 20 mM sodium phosphate buffer containing 1 mM DTT (pH 5.5). The final SDS concentration was 15 mM. For TFE work, samples of the peptide in TFE were prepared by mixing the stock solution with TFE (Sigma-Aldrich) to a final TFE concentration of 40% (v/v). These samples were thoroughly mixed for 5 min and allowed to incubate at 20 °C for 1 h.

For liposome studies, the peptide was dissolved in chloroform containing 20 mg/mL POPC (Avanti Polar Lipids, Alabaster, AL). The sample was then incubated for 1 h and dried under a stream of  $N_2(g)$ . The lipid film was resuspended in ddH<sub>2</sub>O, frozen, and lyophilized overnight. The final peptide-containing liposomes were reconstituted in 20 mM sodium phosphate and 1 mM DTT (pH 5.5) to a final peptide:lipid concentration ratio of 20  $\mu$ M:2.5 mM, followed by five cycles of freezing and thawing. The suspension was extruded through 100 nm polycarbonate membranes and clarified by centrifugation to remove any residual large liposomes. Samples were kept on ice for no more than 24 h prior to use.

**CD Spectroscopy.** Far-UV (far-ultraviolet) CD spectra were recorded in a 2 mm cuvette using a Jasco J-810 spectropolarimeter (Jasco, Tokyo, Japan) at 20 °C and are an average of four scans, using a scan speed of 50 nm/min. A 1 nm bandwidth and a 0.1 nm data pitch were used, with a response time of 1 s. The peptide concentration was 10  $\mu$ M for standard spectra and between 2 and 30  $\mu$ M for concentration dependence studies in TFE and SDS. Spectra were buffer corrected, smoothed using the negative exponential method, and normalized to mean residue ellipticity ( $[\theta]$ ) using the equation

$$[\theta] = (100\theta)/(cnl)$$

where  $[\theta]$  is the molar ellipticity (degrees square centimeter per decimole),  $\theta$  is ellipticity (millidegrees),  $c$  is the protein concentration (millimolar),  $n$  is the number of residues in the peptide, and  $l$  is the path length (centimeters). For all far-UV CD analyses,  $n = 30$  and  $l = 0.2$  cm.

A quantitative estimation of the secondary structural content of the TMD peptide was made using CDPro,<sup>25</sup> which compares the peptide's CD spectra with those of known protein structures. A 43-protein reference set (SP43) with a wavelength

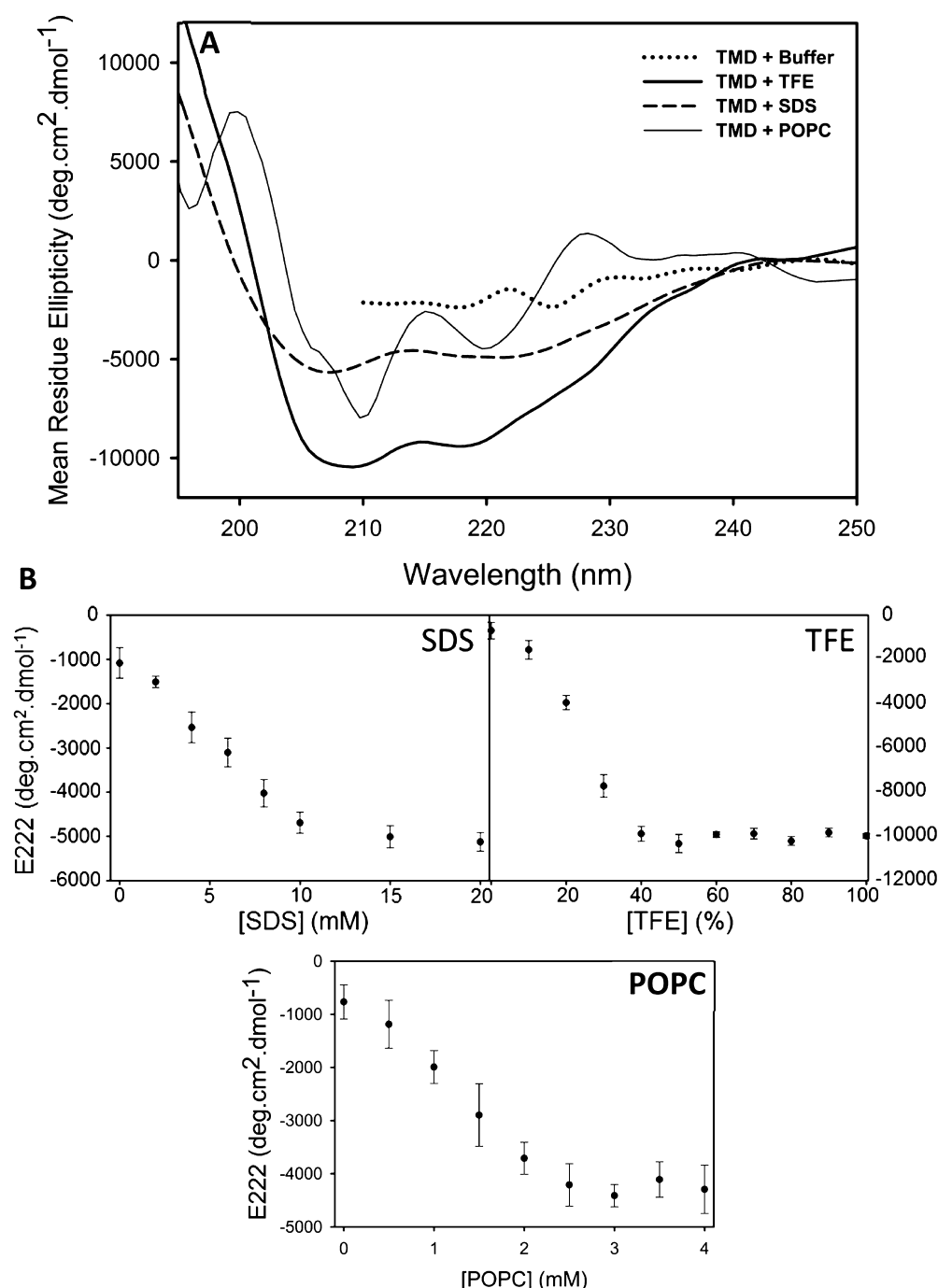


**Figure 2.** Membrane mimetics induce the  $\alpha$ -helical secondary structure of the CLIC1 TMD peptide. (A) Far-UV CD spectra were recorded in buffer (dotted), 40% (v/v) TFE (thick solid), 15 mM SDS micelles (dashed), and 2.5 mM POPC (thin solid). In solution, the peptide is unstructured. Upon addition of TFE, SDS, and POPC, the peptide assumes an  $\alpha$ -helical secondary structure. (B) The helical content of 15  $\mu$ M peptide is maximal at 40% (v/v) TFE, 16 mM SDS, and 2.5 mM POPC, after which no further increase in helicity is observed. The buffer consisted of 20 mM sodium phosphate, 1 mM DTT, and 0.2% (w/v) NaN<sub>3</sub> (pH 5.5).

range of 190–240 nm was used.<sup>26</sup> The standard error of the secondary structural elements was determined from three separate CDPro analyses.

**Fluorescence Spectroscopy.** Fluorescence emission spectra were recorded between 300 and 450 nm using a Perkin-Elmer LS50B luminescence spectrometer (Perkin-Elmer, Waltham, MA) at 20 °C and are an average of three accumulations, using a scan speed of 250 nm/min and 7.5 nm slit widths. An excitation wavelength of 295 nm was used. Samples were analyzed in 20 mM sodium phosphate and 1 mM

DTT (pH 5.5). Spectra were buffer corrected and smoothed using the negative exponential method. The peptide concentration was 10  $\mu$ M for standard spectra and between 2 and 30  $\mu$ M for concentration dependence studies in TFE and SDS. To analyze the effect of oxidation, 10  $\mu$ M peptide was incubated with 2 mM H<sub>2</sub>O<sub>2</sub> for 0–24 h and analyzed as described above.

For quenching studies, the TMD peptide was diluted to 15  $\mu$ M in 0 to 0.4 M acrylamide or sodium iodide (prepared at pH 5.5 with 20 mM sodium phosphate buffer and 1 mM DTT) in the absence and presence of 15 mM SDS or 2.5 mM POPC.

Iodide quenching samples were supplemented with 0.4 to 0 M NaCl to maintain a constant ionic strength. The fluorescence intensity at 345 nm was monitored and analyzed according to the Stern–Volmer relationship:

$$F_0/F = 1 + K_{SV}[Q]$$

where  $F_0$  and  $F$  are the emission intensities in the absence and presence of quencher, respectively,  $[Q]$  is the concentration of quencher, and  $K_{SV}$  is the Stern–Volmer constant. This constant reflects residue accessibility, with low values indicating residues with low levels of exposure and vice versa.<sup>27</sup>

**DTNB Assay.** DTNB [5,5'-dithio(2-nitrobenzoic acid)] is a water-soluble compound used to quantify free thiol (-SH) groups in solution based on their solvent accessibility. The CLIC1 TMD contains a single cysteine residue at position 24. A 20 mM DTNB stock was made in methanol and diluted to a working concentration of 0.2 mM in DTNB buffer [20 mM sodium phosphate and 1 mM EDTA (pH 7.0)] containing 10  $\mu$ M peptide in the absence and presence of 15 mM SDS. In the case of liposome samples, two versions of the DTNB assay were performed: (i) as described above with extrinsic DTNB added to samples and (ii) using DTNB encapsulated within the liposomes. The latter was achieved by including DTNB (final concentration of 0.2 mM) in the reconstitution buffer during liposome preparation (see Sample Preparation). Free DTNB was removed by size-exclusion chromatography on a Sephadex G-25 column equilibrated with DTNB buffer. The aim of these two methods was to probe whether Cys24 is located at the cis or trans face of the membrane mimetic. The concentration of 2-nitro-5-thiobenzoic acid (NTB) was determined spectrophotometrically at 412 nm using an extinction coefficient of 13600 M<sup>-1</sup> cm<sup>-1</sup>.<sup>28</sup> The proportion of free thiols was obtained from the ratio of NTB concentration to peptide concentration.

**Size-Exclusion Chromatography.** Association of the peptide with SDS micelles was probed using size-exclusion chromatography, on the basis that SDS-bound peptide will elute in the void volume while unbound peptide will be retarded. Triplicate samples of 15  $\mu$ M peptide with 15 mM SDS were loaded onto a Sephadex G-25 column (Amersham Biosciences) pre-equilibrated with buffer [20 mM sodium phosphate and 1 mM DTT (pH 5.5)]. Samples containing only 15 mM SDS or 15  $\mu$ M NATA were used as controls for the void volume and total column volume, respectively. Oxidized samples were obtained by incubating 15  $\mu$ M peptide with 2 mM H<sub>2</sub>O<sub>2</sub> and 15 mM SDS for 4 h prior to loading. The elution profiles were corrected for scatter by SDS by running identical samples without peptide and subtracting the two elution profiles. The amount of peptide in each peak was subsequently estimated using the Beer–Lambert law:

$$A = \epsilon_{\lambda}cl$$

where  $A$  is the absorbance at 280 nm,  $\epsilon_{\lambda}$  is the molar extinction coefficient at wavelength  $\lambda$ ,  $c$  is the concentration of the absorbing solution, and  $l$  is the path length of light through the cuvette. For this analysis,  $\epsilon_{\lambda}$  is 5550 M<sup>-1</sup> at 280 nm and  $l$  is 5 mm. The relative percentages of each peak were calculated by dividing the observed peptide concentration by the total peptide concentration. An identical experiment was performed using 2.5 mM POPC liposomes instead of SDS. Peptide bound to the liposomes was detected using a standard Bradford assay. The assay was corrected for scatter contribution by the liposomes using an identical sample in the absence of the TMD peptide.

**Tricine Sodium Dodecyl Sulfate–Polyacrylamide Gel Electrophoresis (SDS–PAGE).** The potential oligomeric state of the TMD peptide in SDS micelles was investigated by gel electrophoresis. A modified Tricine buffer system<sup>29</sup> with a 0.5% SDS gel was used. The peptide (5, 25, or 50  $\mu$ M) was incubated in 20 mM sodium phosphate buffer at pH 7 or 5.5 in the presence of 15 mM SDS as described. A dimer control was included by incubating samples with 2 mM H<sub>2</sub>O<sub>2</sub> in the absence of  $\beta$ -mercaptoethanol, thereby inducing the formation of a Cys24–Cys24 disulfide bond between the two peptides. The samples were boiled for 5 min before being loaded onto a 16% polyacrylamide gel. The gels were run and stained according to the method of Schagger and von Jagow.<sup>29</sup> Silver staining was performed using the SilverQuest kit (Life Technologies, Carlsbad, CA), according to the manufacturer's instructions. The peptide was sized using a Spectra multicolor low-range molecular marker (Fermentas, Glen Burnie, MD).

## RESULTS

**Secondary Structure Content.** The far-UV CD spectra of the TMD peptide in aqueous buffer, TFE, SDS micelles, and POPC liposomes are shown in Figure 2. In solution, the peptide is relatively unstructured. Upon addition of TFE, SDS micelles, or POPC liposomes, the CD spectra exhibit two minima near 208 and 222 nm, which is characteristic of a predominantly  $\alpha$ -helical conformation. POPC spectra displayed an additional maximum at  $\sim$ 228 nm that can be attributed to aromatic side chains adopting an ordered conformation.<sup>26</sup> The molar ellipticity of the TMD peptide in TFE is substantially higher than that in either SDS micelles or POPC liposomes. This suggests that a greater proportion of peptide assumes an  $\alpha$ -helical conformation under these conditions compared to a micellar/vesicle environment. Quantitative analysis using CDPPro shows that the  $\alpha$ -helical content increases substantially, from 18% ( $\pm$ 5%) in buffer to 64% ( $\pm$ 8%) in TFE, 59% ( $\pm$ 10%) in SDS, and 56% ( $\pm$ 9%) in POPC. In contrast, the amount of  $\beta$ -structures in buffer ( $23 \pm 4\%$ ) was reduced 4-fold following the addition of TFE ( $9 \pm 2\%$ ), SDS ( $7 \pm 3\%$ ) and POPC ( $11 \pm 6\%$ ). The amount of unordered structure decreased similarly, with less than 22% ( $\pm$ 9%), 29% ( $\pm$ 7%), and 31% ( $\pm$ 11%) present in TFE-, SDS-, and POPC-containing samples, respectively. The  $\alpha$ -helical content increased with increasing TFE and SDS concentrations, reaching a maximum at 40% (v/v) TFE or 16 mM SDS (Figure 2B). The NRMSD values for the analysis were 0.095 (TFE), 0.11 (SDS), and 0.17 (POPC). The thermal stability of the peptide was also analyzed by measuring the CD spectra in 40% TFE or 15 mM SDS at increasing temperature (Figure S1 of the Supporting Information). The unfolding was shown to be fully reversible but yielded a linear loss of ellipticity rather than a defined unfolding transition. The sequential, rather than simultaneous, disruption of amide hydrogen bonds resulting in this behavior is characteristic of transmembrane helices<sup>30</sup> and indicates unfolding reactions that are local and transient.

**Tertiary Structure.** The TMD peptide contains a lone tryptophan residue at position 35 that can be used as a reporter of local tertiary structural changes. In solution, the peptide exhibits a fluorescence emission spectrum typical of a solvent-exposed tryptophan with a moderately low emission intensity and an emission maximum wavelength ( $\lambda_{\text{max}}$ ) of 355 nm (Figure 3). In the presence of TFE, the emission intensity was reduced by  $\sim$ 25% without altering the  $\lambda_{\text{max}}$ , suggesting that the TFE-induced acquisition of secondary structure is not



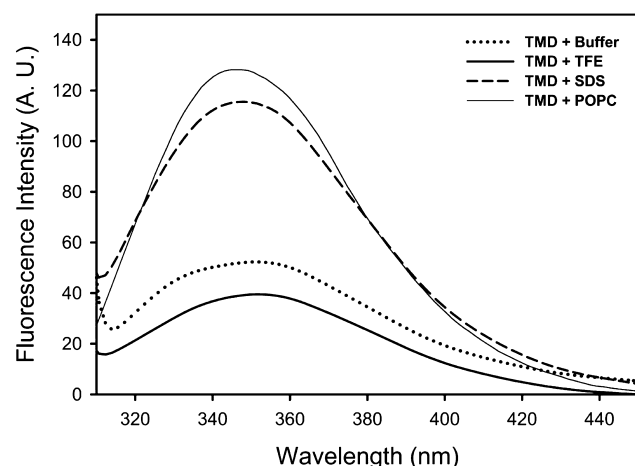


**Figure 3.** Tertiary structure of the CLIC1 TMD peptide. Tryptophan fluorescence emission spectra were recorded in buffer (dotted), 40% (v/v) TFE (thick solid), 15 mM SDS micelles (dashed), and 2.5 mM POPC (thin solid). In solution and in TFE, the peptide emits maximally at 355 nm whereas SDS and POPC induce both a blue-shifted  $\lambda_{\text{max}}$  (343 nm) and a 3-fold increase in emission intensity. This indicates that Trp35 becomes located in a hydrophobic environment, presumably inserted into the SDS micelles or POPC liposomes. The buffer consisted of 20 mM sodium phosphate, 1 mM DTT, and 0.2% (w/v)  $\text{NaN}_3$  (pH 5.5).

accompanied by tertiary packing interactions. SDS and POPC, however, induced both a blue-shifted  $\lambda_{\text{max}}$  (343 nm) and a 3-fold increase in emission intensity. This indicates that, in the presence of SDS or POPC, Trp35 of the TMD peptide is located in a hydrophobic environment, presumably inserted into the SDS micelles or POPC liposomes. The local environment of Trp35 may also, however, be influenced by quaternary interactions in addition to interaction with the SDS micelles or POPC liposomes, particularly if Trp35 is located at or near an oligomer interface.

Under oxidizing conditions, the emission spectra of Trp35 respond in a manner that correlates well with the proposed solvent accessibility of the peptide in the various membrane mimetics (Figure 4). Oxidation of the indole ring to oxyindole quenches Trp35 fluorescence on the basis of solvent accessibility over time, with little to no quenching observed in SDS, minimal quenching in POPC (~5–10%) and TFE (~15%), and substantial quenching in solution (~50%) over 24 h. This likely reflects the nature of the mimetic, with the peptide being inserted into the POPC liposomes or SDS micelles and partially shielded by the TFE. This correlates well with the blue-shifted  $\lambda_{\text{max}}$  in POPC liposomes and SDS micelles and acts as confirmation of insertion. The observed reduction in Trp35 fluorescence in POPC at increasing  $\text{H}_2\text{O}_2$  concentrations is likely a result of a small population of free peptide, with no change in fluorescence reduction observed over time.

**Solvent Accessibility of Trp35 and Cys24 in POPC Liposomes and SDS Micelles.** The association of the TMD peptide with the SDS micelles was probed using size-exclusion chromatography. The underlying basis was that micelle-associated peptide would elute in the void volume while free peptide would be retarded by the resin (Figure 5A). Approximately 66% of the total peptide eluted with the SDS micelles (Figure 5B), suggesting that a large population of the peptide interacts with the mimetic. The reduced monomer and

oxidized dimer forms of the TMD were also identified in the absence of SDS (Figure 5C). The peptide was also shown to interact with POPC liposomes (Figure 5D), with most of the peptide coeluting with the liposomes. The total amount of peptide detected using the Bradford assay in the presence of POPC is comparable to that in the absence of the mimetic (Figure S3 of the Supporting Information). To determine whether the interaction between the TMD peptide and SDS micelles or POPC liposomes involves peripheral association or insertion, dynamic fluorescence quenching with acrylamide or iodide and a DTNB assay were conducted. Both acrylamide and iodide were chosen as complementary probes because of the ability of acrylamide to partially penetrate the interior of SDS micelles,<sup>27</sup> while iodide is excluded on the basis of its charge. Panels A and B of Figure 6 as well as Figure S4 of the Supporting Information show the Stern–Volmer constants ( $K_{\text{SV}}$ ) obtained using acrylamide and iodide, respectively. This constant reflects residue accessibility, with low values indicating residues with low levels of exposure and vice versa.<sup>27</sup> In the absence of SDS micelles, both acrylamide ( $K_{\text{SV}} = 15.35 \text{ M}^{-1}$ ) and iodide ( $K_{\text{SV}} = 3.52 \text{ M}^{-1}$ ) quenching yield Stern–Volmer constants that are comparable to the values for free NATA in solution (16.15 and  $3.88 \text{ M}^{-1}$ , respectively). Upon addition of SDS micelles, a 3-fold reduction in solvent accessibility occurs, clearly indicating that Trp35 is protected from quenching by the micelles. Acrylamide quenching in the presence of POPC liposomes shows a similar reduction in  $K_{\text{SV}}$  values (15.35 and  $7.01 \text{ M}^{-1}$  in the absence and presence of POPC, respectively) (Figure 6A). A similar trend was observed using the DTNB assay, with an ~40% reduction in the fraction of free thiols following the addition of SDS micelles (Figure 6C). This suggests that Trp35 and Cys24 are fully and partially solvent excluded in the presence of SDS micelles, respectively (Figure S5 of the Supporting Information). A dual DTNB assay was employed in the case of POPC liposomes, whereby samples contained either extrinsic DTNB or DTNB encapsulated within the liposomes. The purpose of these two methods was to probe whether Cys24 was located at the cis (outer) or trans (inner) face of the liposomes. The data shown in Figure 6D suggest that a large proportion (~65%) of Cys24 reacts with the encapsulated DTNB reagent, whereas only 30–35% of the residues react with extrinsic DTNB. These combined values correlate with the total reactivity of the peptide in buffer (~100%).

#### Concentration Dependence of Secondary Structure.

The concentration-dependent acquisition of secondary structure was also probed in an attempt to identify any oligomerization events. The normalized  $E_{222}$  values from peptide samples incubated in TFE showed little change over a wide range of peptide concentrations (Figure 7A). In the presence of SDS micelles, however, a 2-fold increase in molar ellipticity was observed (Figure 7A). This may be due to either the increased helical content or a positive shift in the population of peptides assuming helical structure. These data suggest that the TMD peptide associates in a concentration-dependent manner and forms the basis for subsequent investigations of its oligomeric state.

#### Oligomerization of the CLIC1 TMD in SDS Micelles.

On the basis of the observed concentration-dependent secondary structure of the peptide, Tricine SDS–PAGE was conducted to identify potential oligomeric species in the presence of detergent micelles. The use of SDS–PAGE to monitor transmembrane domain association has been well-

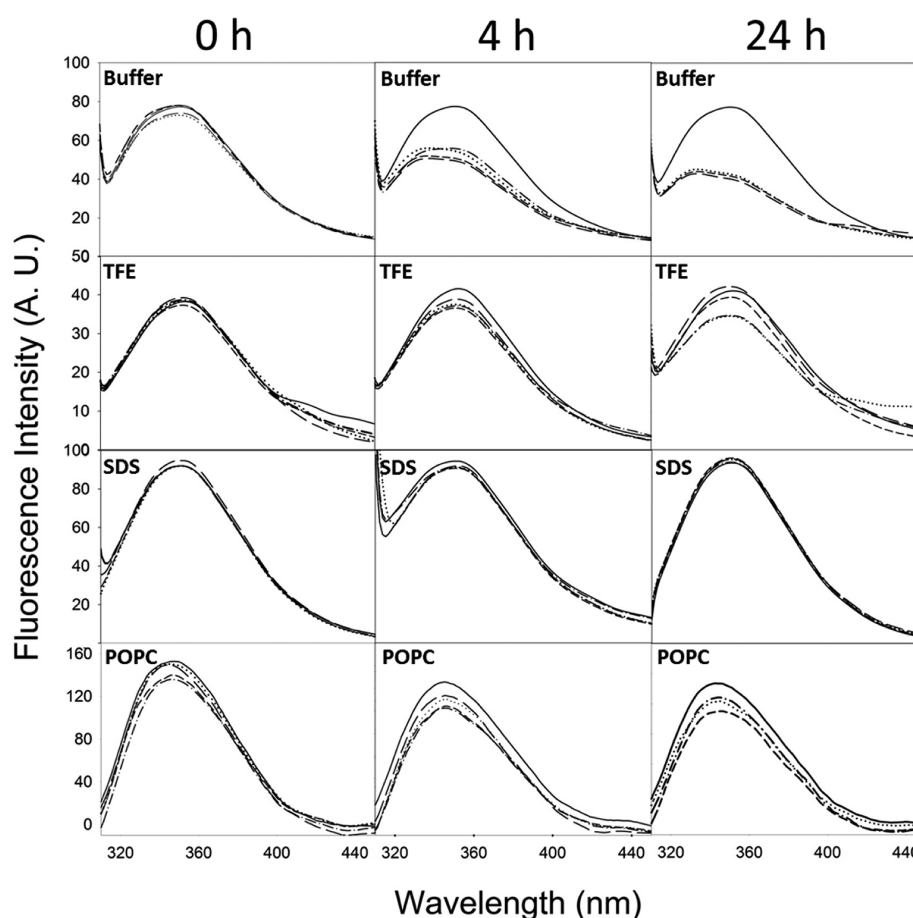


**Figure 4.** Oxidation quenches the fluorescence of Trp35 on the basis of solvent exposure. Samples were analyzed by fluorescence following the addition of 0 (solid), 0.5 (dash dotted), 1 (medium dash), 1.5 (short dash), or 2 mM H<sub>2</sub>O<sub>2</sub> (dotted) in buffer only (top panels), 40% (v/v) TFE (top middle panels), 15 mM SDS micelles (bottom middle panels), or 2.5 mM POPC (bottom panels). Oxidation appears to quench Trp35 fluorescence on the basis of solvent accessibility over time, with no quenching observed in POPC or SDS, minimal quenching in TFE (~15%), and substantial quenching in solution (~50%) over 24 h. The buffer consisted of 20 mM sodium phosphate, 1 mM DTT, and 0.2% (w/v) NaN<sub>3</sub> (pH 5.5).

documented.<sup>31,32</sup> The data shown in Figure 7C show two bands of ~6.9 and ~10.2 kDa across all peptide concentrations tested. These are consistent with a homodimer and homotrimer of the ~3.4 kDa TMD peptide, respectively. Comparison with the disulfide-linked oxidized control sample confirms that the band at 6.9 kDa represents a stable dimeric species. At least 90% of the control peptide was shown to form a disulfide-linked dimer (Figure S2 of the Supporting Information). The absence of a band at 3.4 kDa suggests that the majority of the peptide exists as a dimer/trimer under the conditions tested. Smearing of the peptide band was evident at high peptide concentrations in the absence of aggregation, which suggests an equilibrium between the dimer and higher-order oligomers.<sup>33,34</sup> This is consistent both with the concentration-dependent CD signal and with the blue-shifted fluorescence at high peptide concentrations (Figure 7B). Interestingly, the migration patterns were independent of pH, denaturation, and reducing conditions. This agrees well with the reversible thermal denaturation (Figure S1 of the Supporting Information) and suggests that the helix–helix interactions between TMD peptides are noncovalent.

## DISCUSSION

Membrane-bound CLIC1 plays key roles in cell signaling, homeostatic, and apoptotic processes.<sup>35–37</sup> Despite its physiological relevance, the structure of the membrane-bound form of CLIC1 is yet to be determined. In particular, the structural transition of the transmembrane domain (TMD) during membrane insertion is not well studied. Here we report the secondary, tertiary, and quaternary structural changes in the CLIC1 TMD as it partitions between an aqueous and membrane-mimicking environment. The use of synthetic TMD peptides as models for investigating the structure, assembly, and folding of membrane proteins has been well documented.<sup>38,39</sup>

In the presence of membrane mimetics, the TMD undergoes a dramatic structural rearrangement to form an  $\alpha$ -helix. This conformation is consistent with the predicted membrane conformation of the TMD. The dependence of the secondary structure on both TFE and SDS concentration suggests that one conformation (the unstructured peptide) is progressively depopulated in favor of another (the helical peptide).<sup>40</sup> This transition from unstructured to helical is consistent with the membrane partitioning of a peptide in its transmembrane conformation.<sup>41</sup>

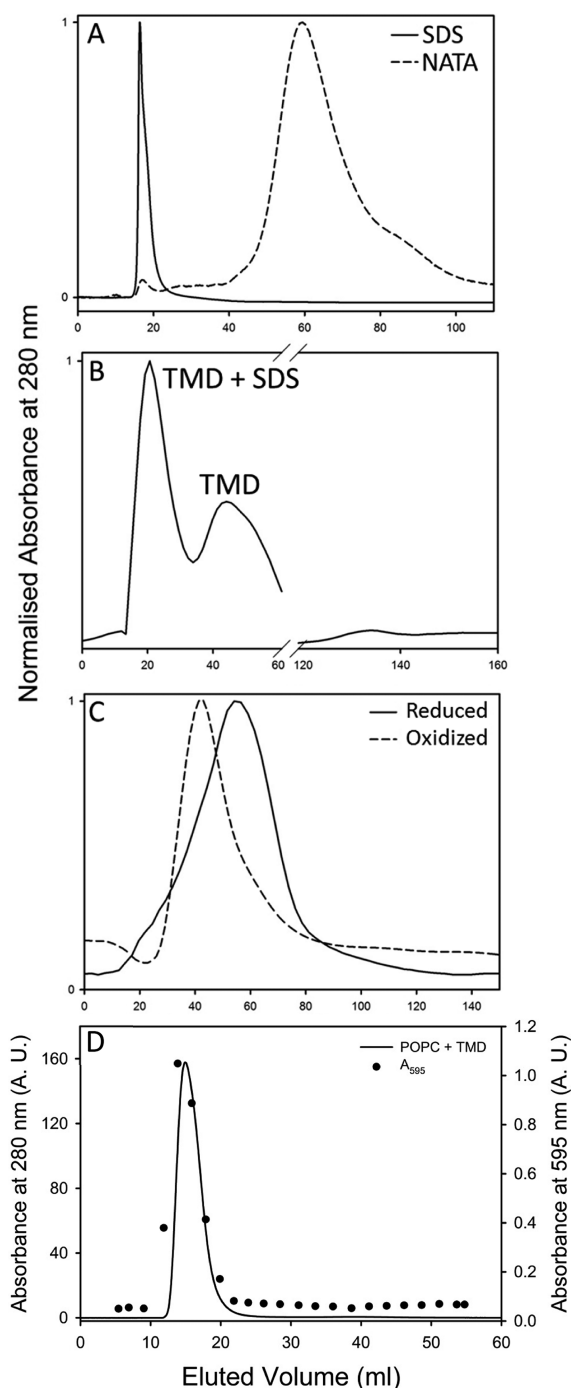


**Figure 5.** CLIC1 TMD peptide associates with SDS micelles and POPC liposomes. (A) Samples containing only SDS and only NATA were used to determine the void volume and total column volume, respectively. (B) A mixture containing 20  $\mu$ M TMD peptide in 15 mM SDS was analyzed on a Sephadex G25 size-exclusion column to determine whether the peptide interacts with SDS micelles. The data show that 66% of the TMD peptide coelutes with the SDS micelles in the void volume. The profile shown has been corrected for scatter contribution by SDS. (C) Control sample containing only the reduced (solid) or oxidized (dashed) TMD peptide in buffer. (D) An identical assay was conducted using POPC liposomes, with the peptide-containing fractions detected using a Bradford assay. The Bradford assay was corrected for the contribution by liposome scatter using an identical sample without the TMD peptide. The buffer consisted of 20 mM sodium phosphate, 1 mM DTT, and 0.2% (w/v)  $\text{NaN}_3$  (pH 5.5).

The membrane-mimetic effect of TFE is caused by an increase in the order of the solvent, making solvent–peptide interactions energetically unfavorable and subsequently promoting interactions between the peptide backbone (i.e., secondary structure).<sup>42</sup> However, isotropic solvents such as TFE lack the chemical and structural heterogeneity of lipid bilayers. In addition, TFE disrupts tertiary and quaternary contacts,<sup>43</sup> explaining the concentration independence of the peptide in TFE. The use of SDS micelles partially circumvents these issues by providing a heterogeneous environment with a polarity that more closely matches that of lipid bilayers.<sup>44</sup> Detergent micelles do, however, exist in equilibrium with detergent monomers and may thus form a hydrophobic surface that does not require insertion of the peptide. This necessitated the inclusion of the lipid bilayer (POPC) system, given that micelles are as likely to form around a peptide as a peptide is to insert into a preexisting micelle.

Fluorescence quenching studies indicate that the acquisition of secondary structure in the presence of SDS and POPC correlates with the insertion of the peptide into SDS micelles and POPC liposomes. Whether these events occur sequentially or in parallel remains unknown, although the two-state folding model of Popot and Engelman<sup>2</sup> tends to favor a sequential mechanism. In this study, the data show that the TMD alone is sufficient to promote membrane insertion in the absence of a signal peptide. This is in line with the work of Singh and Ashley,<sup>45</sup> which showed that the truncated N-domain of CLIC4 was capable of directing membrane insertion in the absence of the C-domain and large portions of the N-domain.

The spatial relationship between the micelles and the peptide is proposed in Figure S5 of the Supporting Information, corresponding to an orientation in which Trp35 is buried near the middle of the micelle. This compares favorably with its expected location within lipid bilayers, determined using brominated phospholipids.<sup>17</sup> Given the average internal diameter of SDS micelles (3–5 nm)<sup>46</sup> and the propensity for helices to extend in membrane environments,<sup>47</sup> the peptide may well be protruding from the micelles rather than being fully inserted (Figure S5A–C of the Supporting Information). The partial reactivity of Cys24 with DTNB confirms that a fraction of the micelle-associated peptide exhibits a protruding N-terminus. This is in line with the findings of Singh and Ashley<sup>45</sup> as well as work comprising FLAG epitopes<sup>14</sup> and terminally directed antibodies.<sup>15</sup> Interestingly, our data suggest that a large proportion (~70%) of the peptide is found in an orientation where Cys24 is exposed to the trans face of the membrane. This correlates with its expected location in the membrane<sup>45</sup> and is consistent with a transmembrane region that moves from the cytoplasm and inserts across an intracellular membrane.

Upon oxidation, wild-type CLIC1 undergoes a structural rearrangement stabilized by the formation of an intramolecular disulfide bond between Cys24 and Cys59.<sup>8</sup> This conformation is thought to promote membrane binding and insertion by increasing the hydrophobic surface area. The insertion of the CLIC1 TMD into SDS micelles and POPC liposomes was observed under reducing conditions and in the absence of Cys59. In addition, work performed using a C24S mutant has shown that the acquisition of helical structure does not require the presence of Cys24.<sup>57</sup> Therefore, the formation of an intramolecular disulfide between Cys24 and Cys59 and the resultant dimerization of full-length CLIC1<sup>8</sup> is unlikely to play a key role in the binding/insertion process. This is supported by

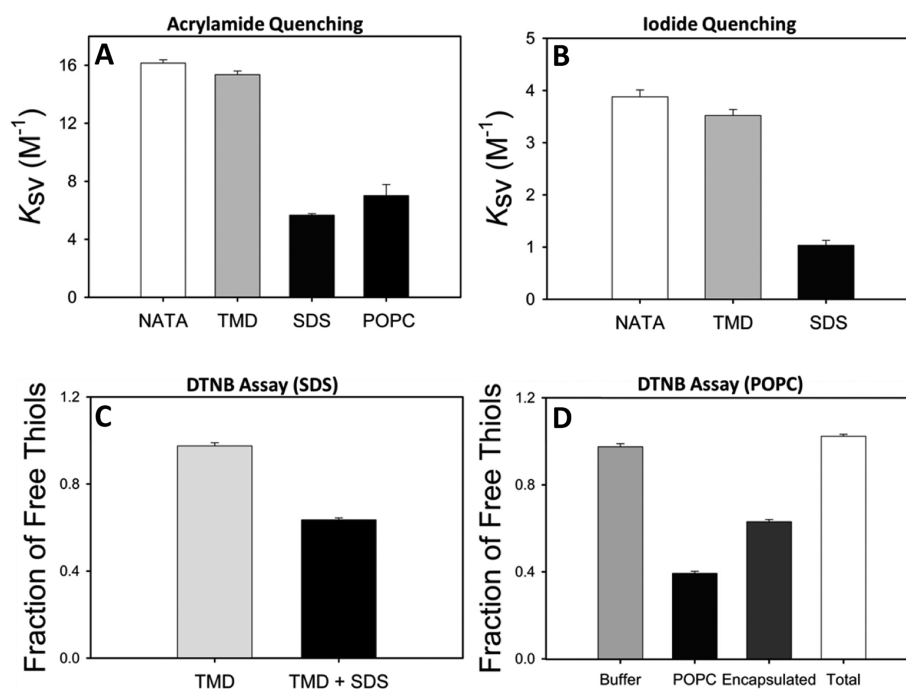


**Figure 6.** Solvent accessibility of the CLIC1 TMD peptide in SDS micelles and POPC liposomes. Dynamic acrylamide (A) and iodide (B) quenching and a DTNB assay (C and D) were performed in the absence and presence of 15 mM SDS or 2.5 mM POPC. In panel D, “buffer” refers to free TMD peptide in solution, “POPC” refers to external DTNB, and “encapsulated” refers to encapsulated DTNB. The buffer consisted of 20 mM sodium phosphate, 1 mM DTT, and 0.2% (w/v)  $NaN_3$  (pH 5.5) (Quenching) or 20 mM sodium phosphate, 1 mM EDTA, and 0.2% (w/v)  $NaN_3$  (pH 6.0) (DTNB Assay).

the fact that not all CLICs and CLIC homologues have a redox-active cysteine at their active sites.<sup>48</sup> Oxidation did, however, have a negative effect on the fluorescence emission of Trp35, consistent with reports of indole degradation by hydrogen peroxide.<sup>49</sup> This not only acts as a means of assessing solvent exposure, because buried tryptophans are inaccessible to  $H_2O_2$ , but also shows that care must be taken when using oxidation to study membrane insertion of CLIC1.<sup>17,50</sup>

In addition to oxidation, low pH has been implicated as a major driving force in membrane binding and/or insertion by both lowering the stability<sup>22</sup> and enhancing the flexibility<sup>23</sup> of the N-domain. This is thought to reduce the energy barrier required to expose and refold the TMD for membrane insertion. This pH dependence is due to the protonation and subsequent disruption of a stabilizing electrostatic network across the protein<sup>51,52</sup> as it moves from the cytosol (pH ~7.4) to the membrane surface (pH ~4–6). This network comprises residues not contained within the TMD, accounting for the pH insensitivity of the peptide’s structure and self-association. This highlights the fact that membrane insertion and dimerization of the TMD itself is likely a pH-independent process, although pH may affect both the exposure of the TMD to the membrane and its ion conducting activity.<sup>21,23</sup> The pH-induced intermediate<sup>22</sup> and the oxidized dimer<sup>8</sup> of full-length CLIC1 are thought to expose hydrophobic regions of the protein, including the TMD. This not only facilitates membrane–protein interactions but also promotes protein–protein interactions (i.e., oligomerization).

Given that CLIC1 contains a single TMD, subsequent oligomerization is required to form a functional pore. This process, which completes the two-step folding model, has been poorly characterized in CLIC1 and forms the basis of much debate. The dimeric and trimeric TMD species identified here

form under reducing conditions, again suggesting that oxidation is unlikely to play a role in this process. The poor staining of the trimeric species using Coomassie staining suggests that the dimer is likely the predominant species. The absence of the monomeric species coupled with data from size-exclusion chromatography (Figure 5) is troubling but may be a result of diffusion of the small peptide out of the gel coupled with poor staining by either Coomassie or silver staining methods. Alternatively, the peptide may display anomalous migration in the SDS–PAGE gel. This phenomenon has been observed for transmembrane peptides,<sup>58,59</sup> where monomeric species were shown to migrate as a dimer. In this study, then, the “dimer” bands may in fact represent the monomer while the “trimer” bands are likely representative of the true dimer. The smearing evident at high peptide concentrations does suggest that an equilibrium exists between the dimer and higher-order oligomers. This highlights possible differences in the thermodynamic stabilities of these species.

A dimer or trimer alone is unlikely to form an ion-conducting pore. Studies by Warton et al.<sup>21</sup> suggest that the dimer may represent a weakly active protopore that subsequently oligomerizes to form the fully active channel. Such behavior has been observed for other proteins that spontaneously insert into membranes, including diphtheria toxin,<sup>53</sup> Bax,<sup>54</sup> and Bcl-x<sub>L</sub>.<sup>7</sup> To date, two models of the functional CLIC1 channel have been proposed. Singh<sup>55</sup> postulates that four protomers, each comprising four TMD helices, interact to form the ion channel. The second model comprises a large channel of at least four subunits, with each subunit comprising six to eight transmembrane helices.<sup>50</sup> Although Förster resonance energy transfer evidence supports this model, the large pore diameter of ~120 Å does not appear to be physiologically feasible, given that other ion-conducting pores have diameters in the range of



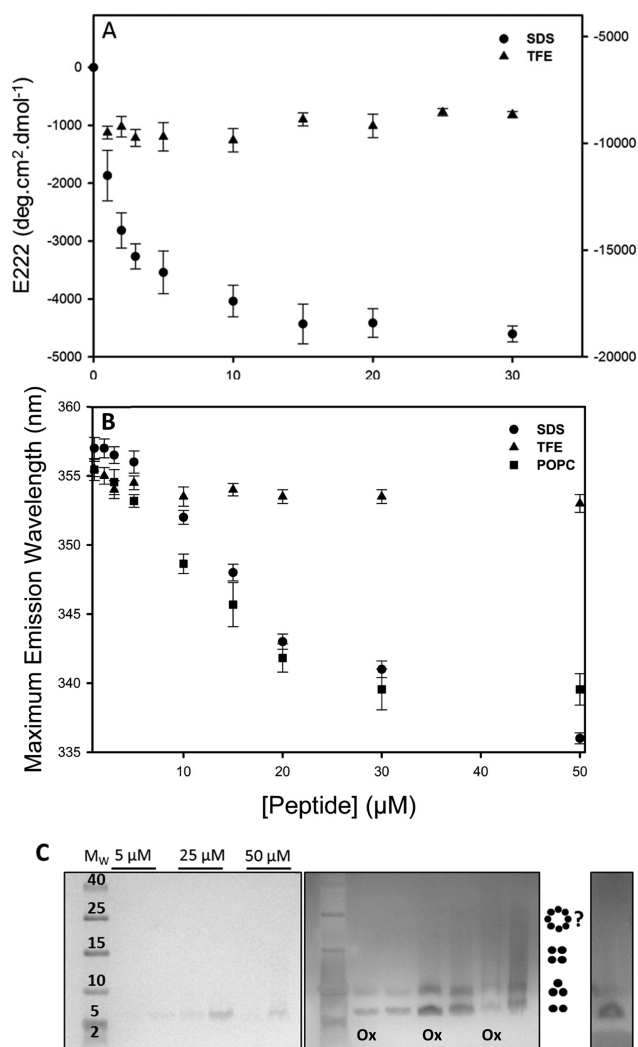


**Figure 7.** Concentration-dependent dimerization of the CLIC1 TMD peptide. (A) Upon conversion to mean residue ellipticity ( $[\theta]$ ), the  $E_{222}$  values from peptide samples incubated in SDS micelles show a 2-fold increase at increasing peptide concentrations whereas those incubated in TFE show no such trend. The right-hand side y-axis represents  $E_{222}$  values in TFE, while that on the left represents those in SDS. (B) The maximal fluorescence emission wavelength also shows a blue shift at increasing peptide concentrations in SDS micelles and POPC liposomes. This suggests that the TMD peptide associates in a concentration-dependent manner in SDS micelles. (C) Stable dimeric (~6.9 kDa) and trimeric (~10.2 kDa) species were subsequently identified using SDS–PAGE under denaturing and reducing conditions. The smearing evident at high peptide concentrations may indicate higher-order tetrameric and octameric species. The gel on the left was stained with Coomassie Brilliant Blue G-250, while that on the right was the same gel stained with silver. The lanes labeled “Ox” refer to the oxidized dimer control at each peptide concentration. An additional dimer control that was oxidized prior to being mixed with SDS is included at the far right.

3–5 Å (chloride channel),<sup>56</sup> being as large as 30 Å for Bax apoptotic proteins.<sup>6,54</sup> Further investigations into the oligomeric states of CLIC1 and its TMD are therefore warranted to gain a better understanding of how this soluble protein comes together to form a functional channel.

In conclusion, the results presented here represent the first analysis of the structure of the CLIC1 TMD in membrane-mimetic environments. The TMD peptide undergoes structural

modifications in the micellar environment, including the acquisition of helical secondary structure and dimerization. We propose that, in the vicinity of membranes, the TMD refolds to form a helix, consistent with the predicted membrane conformation. The single helix then oligomerizes via non-covalent helix–helix interactions to form a membrane-competent protopore complex. Oligomerization does not, therefore, require the C-domain and large portions of the N-domain. However, much work is still needed to clarify both the nature of oligomerization and the forces that drive the peptide to spontaneously associate with micelles and/or membranes. Future work will involve analyzing the kinetics and thermodynamics of the interaction, although the gold standard will always be high-resolution structural data.

## ■ ASSOCIATED CONTENT

### Supporting Information

Thermal unfolding of the CLIC1 TMD peptide in SDS and TFE (Figure S1), oxidation of Cys24 using a DTNB assay at 0 and 4 h (Figure S2), detection of free TMD peptide following size-exclusion chromatography (Figure S3), Stern–Volmer plots for acrylamide and iodide quenching (Figure S4), and a schematic representation of the possible orientations of the TMD peptide in SDS micelles and POPC liposomes (Figure S5). This material is available free of charge via the Internet at <http://pubs.acs.org>.

## ■ AUTHOR INFORMATION

### Corresponding Author

\*E-mail: [heinrich.dirr@wits.ac.za](mailto:heinrich.dirr@wits.ac.za). Telephone: +27 11 7176352. Fax: +27 11 7176351.

### Funding

This work was supported by the University of the Witwatersrand, the South African National Research Foundation (Grants 60810, 65510, and 68898 to H.W.D.), and the South African Research Chairs Initiative of the Department of Science and Technology and National Research Foundation (Grant 64788 to H.W.D.).

### Notes

The authors declare no competing financial interest.

## ■ ABBREVIATIONS

CD, circular dichroism; CLIC1, chloride intracellular channel protein 1; DTNB, 5,5'-dithio(2-nitrobenzoic acid); DTT, dithiothreitol; GST, glutathione transferase; NATA, N-acetyltryptophanamide; POPC, 1-palmitoyl-2-oleoyl-*sn*-glycero-3-phosphocholine; PTM, putative transmembrane domain; SDS, sodium dodecyl sulfate; TFE, 2,2,2-trifluoroethanol; TMD, transmembrane domain of CLIC1 (residues 24–46).

## ■ REFERENCES

- (1) Overington, J. P., Al-Lazikani, B., and Hopkins, A. L. (2006) How many drug targets are there? *Nat. Rev. Drug Discovery* 5, 993–996.
- (2) Popot, J. L., and Engelman, D. M. (1990) Membrane protein folding and oligomerization: The two-stage model. *Biochemistry* 29, 4031–4037.
- (3) White, S. H., and Wimley, W. C. (1999) Membrane protein folding and stability: Physical principles. *Annu. Rev. Biophys. Biomol. Struct.* 28, 319–365.
- (4) Johnson, J. E., and Cornell, R. B. (1999) Amphitropic proteins: Regulation by reversible membrane interactions. *Mol. Membr. Biol.* 16, 217–235.

- (5) van der Goot, F. G., Gonzalez-Manas, J. M., Lakey, J. H., and Pattus, F. (1991) A 'molten-globule' membrane-insertion intermediate of the pore-forming domain of colicin A. *Nature* 354, 408–410.
- (6) Parker, M. W., and Feil, S. C. (2005) Pore-forming protein toxins: From structure to function. *Prog. Biophys. Mol. Biol.* 88, 91–142.
- (7) Thuduppathy, G. R., and Hill, R. B. (2006) Acid destabilization of the solution conformation of Bcl-xL does not drive its pH-dependent insertion into membranes. *Protein Sci.* 15, 248–257.
- (8) Littler, D. R., Harrop, S. J., Fairlie, W. D., Brown, L. J., Pankhurst, G. J., Pankhurst, S., DeMaere, M. Z., Campbell, T. J., Bauskin, A. R., Tonini, R., Mazzanti, M., Breit, S. N., and Curmi, P. M. (2004) The intracellular chloride ion channel protein CLIC1 undergoes a redox-controlled structural transition. *J. Biol. Chem.* 279, 9298–9305.
- (9) Harrop, S. J., DeMaere, M. Z., Fairlie, W. D., Reztsova, T., Valenzuela, S. M., Mazzanti, M., Tonini, R., Qiu, M. R., Jankova, L., Warton, K., Bauskin, A. R., Wu, W. M., Pankhurst, S., Campbell, T. J., Breit, S. N., and Curmi, P. M. (2001) Crystal structure of a soluble form of the intracellular chloride ion channel CLIC1 (NCC27) at 1.4-Å resolution. *J. Biol. Chem.* 276, 44993–45000.
- (10) Ponce, A., Vega-Saenz de Miera, E., Kentros, C., Moreno, H., Thornhill, B., and Rudy, B. (1997) K<sup>+</sup> channel subunit isoforms with divergent carboxy-terminal sequences carry distinct membrane targeting signals. *J. Membr. Biol.* 159, 149–159.
- (11) Cromer, B. A., Morton, C. J., Board, P. G., and Parker, M. W. (2002) From glutathione transferase to pore in a CLIC. *Eur. Biophys. J.* 31, 356–364.
- (12) Berryman, M., and Bretscher, A. (2000) Identification of a novel member of the chloride intracellular channel gene family (CLIC5) that associates with the actin cytoskeleton of placental microvilli. *Mol. Biol. Cell* 11, 1509–1521.
- (13) Duncan, R. R., Westwood, P. K., Boyd, A., and Ashley, R. H. (1997) Rat brain p64H1, expression of a new member of the p64 chloride channel protein family in endoplasmic reticulum. *J. Biol. Chem.* 272, 23880–23886.
- (14) Tonini, R., Ferroni, A., Valenzuela, S. M., Warton, K., Campbell, T. J., Breit, S. N., and Mazzanti, M. (2000) Functional characterization of the NCC27 nuclear protein in stable transfected CHO-K1 cells. *FASEB J.* 14, 1171–1178.
- (15) Proutski, I., Karoulas, N., and Ashley, R. H. (2002) Overexpressed chloride intracellular channel protein CLIC4 (p64H1) is an essential component of novel plasma membrane anion channels. *Biochem. Biophys. Res. Commun.* 297, 317–322.
- (16) Berry, K. L., and Hobert, O. (2006) Mapping functional domains of chloride intracellular channel (CLIC) proteins in vivo. *J. Mol. Biol.* 359, 1316–1333.
- (17) Goodchild, S. C., Howell, M. W., Cordina, N. M., Littler, D. R., Breit, S. N., Curmi, P. M., and Brown, L. J. (2009) Oxidation promotes insertion of the CLIC1 chloride intracellular channel into the membrane. *Eur. Biophys. J.* 39, 129–138.
- (18) Landolt-Marticorena, C., Williams, K. A., Deber, C. M., and Reithmeier, R. A. (1993) Non-random distribution of amino acids in the transmembrane segments of human type I single span membrane proteins. *J. Mol. Biol.* 229, 602–608.
- (19) Arkin, I. T., and Brunger, A. T. (1998) Statistical analysis of predicted transmembrane  $\alpha$ -helices. *Biochim. Biophys. Acta* 1429, 113–128.
- (20) Hunte, C., Screpanti, E., Venturi, M., Rimón, A., Padan, E., and Michel, H. (2005) Structure of a Na<sup>+</sup>/H<sup>+</sup> antiporter and insights into mechanism of action and regulation by pH. *Nature* 435, 1197–1202.
- (21) Warton, K., Tonini, R., Fairlie, W. D., Matthews, J. M., Valenzuela, S. M., Qiu, M. R., Wu, W. M., Pankhurst, S., Bauskin, A. R., Harrop, S. J., Campbell, T. J., Curmi, P. M., Breit, S. N., and Mazzanti, M. (2002) Recombinant CLIC1 (NCC27) assembles in lipid bilayers via a pH-dependent two-state process to form chloride ion channels with identical characteristics to those observed in Chinese hamster ovary cells expressing CLIC1. *J. Biol. Chem.* 277, 26003–26011.
- (22) Fanucchi, S., Adamson, R. J., and Dirr, H. W. (2008) Formation of an unfolding intermediate state of soluble chloride intracellular channel protein CLIC1 at acidic pH. *Biochemistry* 47, 11674–11681.
- (23) Stoychev, S. H., Nathaniel, C., Fanucchi, S., Brock, M., Li, S., Asmus, K., Woods, V. L., Jr., and Dirr, H. W. (2009) Structural dynamics of soluble chloride intracellular channel protein CLIC1 examined by amide hydrogen-deuterium exchange mass spectrometry. *Biochemistry* 48, 8413–8421.
- (24) Killian, J. A., Trouard, T. P., Greathouse, D. V., Chupin, V., and Lindblom, G. (1994) A general method for the preparation of mixed micelles of hydrophobic peptides and sodium dodecyl sulphate. *FEBS Lett.* 348, 161–165.
- (25) Sreerama, N., and Woody, R. W. (2000) Estimation of protein secondary structure from circular dichroism spectra: Comparison of CONTIN, SELCON, and CDSSTR methods with an expanded reference set. *Anal. Biochem.* 287, 252–260.
- (26) Sreerama, N., Vennyaminov, S. Y., and Woody, R. W. (2001) Analysis of protein circular dichroism spectra based on the tertiary structure classification. *Anal. Biochem.* 299, 271–274.
- (27) Eftink, M. R., and Ghiron, C. A. (1981) Fluorescence quenching studies with proteins. *Anal. Biochem.* 114, 199–227.
- (28) Habeeb, A. F. (1972) Reaction of protein sulfhydryl groups with Ellman's reagent. *Methods Enzymol.* 25C, 457–464.
- (29) Schagger, H., and von Jagow, G. (1987) Tricine-sodium dodecyl sulfate-polyacrylamide gel electrophoresis for the separation of proteins in the range from 1 to 100 kDa. *Anal. Biochem.* 166, 368–379.
- (30) Langosch, D., and Arkin, I. T. (2009) Interaction and conformational dynamics of membrane-spanning protein helices. *Protein Sci.* 18, 1343–1358.
- (31) Wigley, W. C., Vijayakumar, S., Jones, J. D., Slaughter, C., and Thomas, P. J. (1998) Transmembrane domain of cystic fibrosis transmembrane conductance regulator: Design, characterization, and secondary structure of synthetic peptides m1-m6. *Biochemistry* 37, 844–853.
- (32) Melnyk, R. A., Partridge, A. W., and Deber, C. M. (2001) Retention of native-like oligomerization states in transmembrane segment peptides: Application to the *Escherichia coli* aspartate receptor. *Biochemistry* 40, 11106–11113.
- (33) Thanassi, D. G., Saulino, E. T., Lombardo, M. J., Roth, R., Heuser, J., and Hultgren, S. J. (1998) The PapC usher forms an oligomeric channel: Implications for pilus biogenesis across the outer membrane. *Proc. Natl. Acad. Sci. U.S.A.* 95, 3146–3151.
- (34) Studer, S., and Narberhaus, F. (2000) Chaperone activity and homo- and hetero-oligomer formation of bacterial small heat shock proteins. *J. Biol. Chem.* 275, 37212–37218.
- (35) Fernandez-Salas, E., Sagar, M., Cheng, C., Yuspa, S. H., and Weinberg, W. C. (1999) p53 and tumor necrosis factor  $\alpha$  regulate the expression of a mitochondrial chloride channel protein. *J. Biol. Chem.* 274, 36488–36497.
- (36) Landry, D. W., Akabas, M. H., Redhead, C., Edelman, A., Cragoe, E. J., Jr., and Al-Awqati, Q. (1989) Purification and reconstitution of chloride channels from kidney and trachea. *Science* 244, 1469–1472.
- (37) Ronnov-Jessen, L., Villadsen, R., Edwards, J. C., and Petersen, O. W. (2002) Differential expression of a chloride intracellular channel gene, CLIC4, in transforming growth factor- $\beta$ 1-mediated conversion of fibroblasts to myofibroblasts. *Am. J. Pathol.* 161, 471–480.
- (38) Aggeli, A., Bannister, M. L., Bell, M., Boden, N., Findlay, J. B., Hunter, M., Knowles, P. F., and Yang, J. C. (1998) Conformation and ion-channeling activity of a 27-residue peptide modeled on the single-transmembrane segment of the IsK (minK) protein. *Biochemistry* 37, 8121–8131.
- (39) Yeagle, P. L., Danis, C., Choi, G., Alderfer, J. L., and Albert, A. D. (2000) Three dimensional structure of the seventh transmembrane helical domain of the G-protein receptor, rhodopsin. *Mol. Vision* 6, 125–131.
- (40) Demchenko, A. P. (2001) Concepts and misconcepts in the analysis of simple kinetics of protein folding. *Curr. Protein Pept. Sci.* 2, 73–98.

- (41) MacKenzie, K. R., Prestegard, J. H., and Engelman, D. M. (1997) A transmembrane helix dimer: Structure and implications. *Science* 276, 131–133.
- (42) Buck, M. (1998) Trifluoroethanol and colleagues: Cosolvents come of age. Recent studies with peptides and proteins. *Q. Rev. Biophys.* 31, 297–355.
- (43) Roccatano, D., Colombo, G., Fioroni, M., and Mark, A. E. (2002) Mechanism by which 2,2,2-trifluoroethanol/water mixtures stabilize secondary-structure formation in peptides: A molecular dynamics study. *Proc. Natl. Acad. Sci. U.S.A.* 99, 12179–12184.
- (44) Tulumello, D. V., and Deber, C. M. (2009) SDS micelles as a membrane-mimetic environment for transmembrane segments. *Biochemistry* 48, 12096–12103.
- (45) Singh, H., and Ashley, R. H. (2007) CLIC4 (p64H1) and its putative transmembrane domain form poorly selective, redox-regulated ion channels. *Mol. Membr. Biol.* 24, 41–52.
- (46) Hierrezuelo, J. M., Aguiar, J., and Ruiz, C. C. (2004) Stability, interaction, size, and microenvironmental properties of mixed micelles of decanoyl-N-methylglucamide and sodium dodecyl sulfate. *Langmuir* 20, 10419–10426.
- (47) Pace, C. N., and Scholtz, J. M. (1998) A helix propensity scale based on experimental studies of peptides and proteins. *Biophys. J.* 75, 422–427.
- (48) Littler, D. R., Harrop, S. J., Brown, L. J., Pankhurst, G. J., Mynott, A. V., Luciani, P., Mandyam, R. A., Mazzanti, M., Tanda, S., Berryman, M. A., Breit, S. N., and Curmi, P. M. (2008) Comparison of vertebrate and invertebrate CLIC proteins: The crystal structures of *Caenorhabditis elegans* EXC-4 and *Drosophila melanogaster* DmCLIC. *Proteins* 71, 364–378.
- (49) Cavatorta, P., Favilla, R., and Mazzini, A. (1979) Fluorescence quenching of tryptophan and related compounds by hydrogen peroxide. *Biochim. Biophys. Acta* 578, 541–546.
- (50) Goodchild, S. C., Angstrom, C. N., Breit, S. N., Curmi, P. M., and Brown, L. J. (2011) Transmembrane extension and oligomerization of the CLIC1 chloride intracellular channel protein upon membrane interaction. *Biochemistry* 50, 10887–10897.
- (51) Achilonu, I., Fanucchi, S., Cross, M., Fernandes, M., and Dirr, H. W. (2012) Role of individual histidines in the pH-dependent global stability of human chloride intracellular channel 1. *Biochemistry* 51, 995–1004.
- (52) Legg-E'silva, D., Achilonu, I., Fanucchi, S., Stoychev, S., Fernandes, M., and Dirr, H. W. (2012) Role of Arginine 29 and Glutamic Acid 81 Interactions in the Conformational Stability of Human Chloride Intracellular Channel 1. *Biochemistry*. 51, 7854–7862.
- (53) Bennett, M. J., Choe, S., and Eisenberg, D. (1994) Refined structure of dimeric diphtheria toxin at 2.0 Å resolution. *Protein Sci.* 3, 1444–1463.
- (54) Garcia-Saez, A. J., Mingarro, I., Perez-Paya, E., and Salgado, J. (2004) Membrane-insertion fragments of Bcl-xL, Bax, and Bid. *Biochemistry* 43, 10930–10943.
- (55) Singh, H. (2010) Two decades with dimorphic Chloride Intracellular Channels (CLICs). *FEBS Lett.* 584, 2112–2121.
- (56) Jentsch, T. J. (2002) Chloride channels are different. *Nature* 415, 276–277.
- (57) Ngubane, C. (2012) The Transmembrane Domain of CLIC1 is Helical in Membrane-Mimetic Environments. Unpublished M.Sc. Dissertation (<http://hdl.handle.net/10539/11477>).
- (58) Walkenhorst, W. F., Merzlyakov, M., Hristova, K., and Wimley, W. C. (2009) Polar residues in transmembrane helices can decrease electrophoretic mobility in polyacrylamide gels without causing helix dimerization. *Biochim. Biophys. Acta* 1788, 1321–1331.
- (59) Rath, A., Glibowicka, M., Nadeau, V. G., Chen, G., and Deber, C. M. (2009) Detergent binding explains anomalous SDS-PAGE migration of membrane proteins. *Proc. Natl. Acad. Sci. U.S.A.* 106, 1760–1765.